LA-UR -86-3115   CONF - 86CC9C7 1οι - - 2

LA-UR--86-3115

DE87 000141

TITLE   LASER NEUTRALIZATION

AUTHOR(S)   Otis G. Peterson, CHM-6

DISCLAIMER

Los Alamos

Los Alamos National Laboratory
Los Alamos, New Mexico 87545

LASER NEUTRALIZATION

Otis Peterson
Chemistry Division
Los Alamos National Laboratory
Los Alamos, New Mexico 87545

September 5, 1986

Laser photodetachment of the excess electron to neutralize relativistic ions offers many advantages over the more conventional collisional methods using gases or thin foils as the neutralization agents. Several of these advantages are delineated in Fig. 3 and will be expanded upon in the rest of this document. Probably the two most important advantages of laser photodetachment are the generation of a compact and low divergence beam, and the production of intense neutral beams at very high efficiency (approximately 90%). The high intensities or high current densities of the neutral beam result from the fixed maximum divergence that can be added to the beam by photodetachment of the charge using laser intensity of fixed wavelength and incident angle. The high neutralization efficiency is possible because there is no theoretical maximum to the neutralization efficiency, although higher efficiencies require higher laser powers and, therefore, costs. Additional advantages include focusability of the laser light onto the ion beam to maximize its efficacy. There certainly is no residual gas left in the particle beam path as is typical with gas neutralizers. The photodetachment process leaves the neutral atoms in the ground state so there is no excited state fluorescence to interfere with the subsequent beam sensing. Finally, since the beams to be neutralized are very high powered, for a large range of neutralization efficiencies the neutral beam can be increased more by increasing the power to the laser neutralizer than by adding an equal amount of power to the primary accelerator.

The neutralization chamber in its conceptional configuration is illustrated in Fig. 4. This chamber must contain the laser beam for a very large number of passes because the small absorption coefficient characteristic of the ion together with the very small density of ions precludes any significant absorption of the beam by the ions. The only measurable loss of the laser photons comes from the multiple reflections within the chamber. Efficient utilization of the laser photons requires that the mirror surfaces have very high reflectivity, between 0.999 and 0.9999, and that the chamber geometry permit a very large number of passes through the chamber to take advantage of the high reflectivity. A very high-powered laser beam is focused onto the axis of the chamber with the beam pointed at an angle such that the beam will not immediately escape out of the entrance aperture. The cylindrical chamber will repeatedly focus the beam back onto the axis, as illustrated in Fig. 5, until

the beam has made many transits through the chamber and finally makes its way back to the entrance aperture and escapes. The unit magnification characteristic of cylinders makes many optical aberrations vanish, which insures faithful replication of the focus on the multiple passes.

The axially integrated intensity as a function of the distance from the axis of the chamber is displayed in Fig. 6 for a large number of Gaussian beams incident on the axis from all angles. The intensity falls off as $1/r$ for large radii but is sharply peaked on the axis where it can effectively neutralize the ion beam. For comparison purposes, the constituent laser beam is displayed together with the Gaussian particle beam.

The laser power required to neutralize the ion beam using the integrated intensity profile as shown in Fig. 6 has been evaluated and is displayed in Fig. 7. The calculation performed to determine the functional relationship displayed in the figure has assumed that the mirror surface has a reflectivity of 0.9999 and that the chamber has been designed to effectively use up all of the incoming laser photons. The calculations were performed to map out the geometric and laser intensity parameter space. It was found that for a large portion of this parameter space there was a minimum in the power required to achieve a fixed neutralization fraction. To achieve this minimum in the laser power required that the laser be tightly focused and that the laser be extremely intense on the axis of the neutralizer. Quantitatively, the characteristic diameter of the laser beam must be smaller than the Gaussian diameter of the particle beam and the neutralization must be near 99% (the transmitted ions, n, must be near 1% of the incident ions, n_0: $n/n_0 = 0.01$). Also displayed in the figure are two less than ideal configurations for comparison purposes. One shows that for a laser beam larger than the particle beam significantly, more laser power is required. The other shows that less than 99% neutralization on axis configurations will asymptote to a lower maximum neutralization fraction. Both of these results appear intuitively correct. There are two important aspects of this figure that must be noted. One is that the laser power is linearly dependent on the particle beam diameter so the results displayed are for a nominal 1-cm beam. The other is that laser power generates a specified neutralization fraction independent of the particle beam current. This latter characteristic is a consequence of the fact that no noticeable number of photons are lost to the neutralization process.

The neutral beam generated by the laser photodetachment has much greater intensities or beam current densities in the far-field on-target than any collisional neutralization method. The comparative intensities are illustrated in Fig. 8 where the contributions of the two classes of neutralizers to the beam divergence are compared. In the figure, the contributions of the neutralizers are illustrated only and the accelerator is assumed to generate an ideal plane wave of zero divergence. It is clear that the peak intensity generated by the laser process is at least five times greater than that of the collisionally neutralized beam. The distribution illustrated for the laser process is characteristic of that obtained from a laser beam polarized in the direction of propagation of the ion beam. The collisional generated curve is representative of the experimentally determined characteristics of such neutralization schemes. The factor of 5 is made up of two components, as delineated in Fig. 9. The first of these is the increase in neutralization from 55%, expected from collisional neutralization, to the value of 90%, which may be

expected from laser processes. The second is the elimination of the high angle wings in the scattering profile which are characteristic of the collisional neutralization. There is a very important distinction between the two neutralization methods that is quite obvious from the figure. The 1/e point for both of the far field distributions are quite similar in value. However, neither of the distributions are Gaussian in shape, in fact they are essentially opposites in character, one with extremely extended wings and the other with a very distinctively sharp cutoff. It is clear that the simple comparison between the beam widths at their 1/e intensity points can generate very misleading conclusions. Since the efficacy of neutral beams in the far field is proportional to the intensity or current density that can be generated at that point, the above comparison illustrated in Fig. 8 and summarized in Fig. 9 is the more valid one.

One of the unique features of the laser photodetachment neutralization is the tunable divergence available from the adjusting of the laser wavelength. By using lasers of longer wavelengths with photon energies closer to the photodetachment threshold of 0.75 eV, the excess energy imparted to the ejected electron is reduced, thereby reducing the neutral beam divergence. Unfortunately, as this wavelength is increased, the absorption cross section decreases, requiring proportional increases in laser energy. The magnitude of these effects are illustrated in Fig. 10 where the divergences are compared, at fixed incidence angle, for excitation wavelengths corresponding to nominal reductions in the absorption cross section. Each factor-of-two reduction in the cross section will require a nominal factor-of-two increase in the laser power. This yields a rough estimate of the costs of generating tightly focused beams. Since the beam intensity in the far field is inversely proportional to the square of the divergence, the ratio of the intensity to the laser power is still increasing even at the smallest cross section for which the calculation was performed.

Significant progress has been made toward developing the technology for photodetaching the excess electron on the relativistic ion as summarized in Fig. 11. An optical transport code has been written and verified which can now be used to design and evaluate neutralizer geometries. The code has been verified on spherical geometries where the design results can be compared to analytic results. The initial designs that have been generated by this code have demonstrated that 10's passes can be put into a chamber which has a characteristic dimension which is 15 times the laser beam diameter. It was found that the chamber had to have a 5% eccentricity elliptical cross section to keep the laser beam from walking out of the particle beam apertures.

The results of the design calculations are displayed in Figs. 12, 13, and 14. The points in Fig. 12 are the places where the central ray of the laser beam touches the chamber surface on the more than one thousand reflections that occur inside the chamber. Also displayed is the laser beam entrance aperture which is also the size of that beam. The reflector is seen to be nearly spherical with just enough elliptical eccentricity (5%) to turn the step wise motion of the beam intersections around before the beam marches out of the particle beam apertures. It is seen that the reflection spots become denser in the turn around regions but the chamber surface is quite uniformly covered.

The oblate ellipsoidal geometry of the chamber has some distinctive properties. One of these is illustrated in Fig. 13 where it is seen that the beams alternately pass through the elliptical foci. This means that the neutralization occurs predominantly in two locations. There is a significant advantage to the two-point neutralization because any space charge-induced divergence should be cancelable by application of an external field. The axial view of the chamber is displayed in Fig. 14 which illustrates the fact that the central ray of every beam passes through the axis, proving that the highest intensity in the chamber is indeed on the axis of the neutralizer.

Now that this code is operational, there are several important issues that can be addressed and answered, several of which are listed in Fig. 15. Designs of many different geometries can be prepared and compared. Maximum beam packing density designs can be obtained and the relationship between the maximum number of beam passes and the chamber size determined. The code has the option to propagate as many as five rays to more fully characterize the laser beam. Exercising this option will permit evaluation of the focusing and aberration characteristics of the chamber. In addition, the tolerances required in the manufacture, and the input conditions required to obtain maximum utilization of the device, both can be evaluated.

Since the success of the laser neutralization is so critically dependent on the generation of large-area, ultra-high-reflectivity mirrors, a program has been initiated to develop the metrology for evaluating these mirrors. To this end, two devices have been set up: a calorimeter to measure the absolute absorption loss of any mirror and a ring-down device to measure the total reflectivity of high-reflectivity mirrors. The schematic of the calorimeter is shown in Fig. 16. It consists of a vacuum chamber in which are mounted two mirrors on identical substrates, one of which will be exposed to laser illumination and the other which has a resistance heater bonded to its surface. The mirrors are specially coated on thin, low thermal mass substrates to improve the sensitivity of the measurement. The sample mirror is then exposed to radiation from a 10-W laser. By maintaining the second mirror, which is in an identical environment, at the same temperature as the first using the resistive heater, the laser power absorbed in the first mirror can be accurately determined. Measurement sensitivity of 10 µW has been obtained which yields 1-ppM results. Sample mirrors have been measured to have absorption losses in the 80- to 170-ppM range which is close to that which would be acceptable for the neutralizer application.

To measure the total reflectivity or total mirror loss which is critical to the neutralizer performance, a ring-down device has been assembled. The accuracy of reflectivity measurements which compare the reflected intensity to the incident intensity becomes unacceptable when the mirrors have reflectivities of 99% or greater. To make measurements on higher reflectivity mirrors, new techniques have had to be developed which include the ring down device which is shown schematically in Fig. 17. This measurement technique uses the fact that light can be trapped within a resonant device for measureable periods of time if the losses within the resonator are sufficiently low. The limits on the technique include switch off times for the laser illumination and the reflectivity of the resonator mirrors which must be within an order of magnitude of the sample mirror. An example of data taken on a ring down device is shown in Fig. 18. It is seen that the temporal decay of the light in the

resonator is very accurately exponential over several characteristic lifetimes. This device is admirably suited for measuring reflectivities in the range between 0.999 and 0.9999.

The photos in Figs. 19 and 20 display the laboratory in which both instruments are situated, the calorimeter being a vacuum box located in the back of the room and the ring-down device located on the closer optical table. The Nd:YAG laser powering both instruments is also on the optical table. The comments made in Fig. 21 summarize the status of these instruments at this present time.

A new idea for neutralizing ion beams has been generated recently which combines some of the good features of both the laser and collisional schemes. It employs laser-generated atomic-excited-states to collisionally neutralize the ions. The excited states of the atoms should have collisional cross sections as much as 10 times that of the ground-state atoms. In addition, because of the very high atomic optical absorption cross sections, much less laser power should be required to maintain the required excited-state populations. The result as stated in Fig. 22 is that the new scheme should require almost 10 times less laser power and the effective divergence of the neutral beam should be greatly reduced because 10 times less collision partners are required.

The schematic of the proposed process is displayed in Fig. 23. An atomic beam is projected across the path of the ion beam. The area of intersection is illuminated on both sides with intense laser radiation. The illumination is scaled to replenish fluorescence losses and to ensure an adequate density of excited atoms. Because of the high absorption cross section of the ground-state atoms, the interaction region will be optically thick and the fluorescence within the medium will be trapped.

The potential advantages of this excited atom neutralization are summarized in Fig. 24. The cross sections for collisional electron detachment should increase by as much as an order of magnitude. Such enhancements of the cross sections has been observed at low energies but must be verified at high energy for this application. The increased cross section permits a proportional reduction in the atom density required to achieve the neutralization. The lower density of scattering atoms should significantly reduce the high-angle scattering which would greatly increase the intensity on target in the far field.

The amount of laser illumination would be significantly reduced from that required to do direct photodetachment of the ion's electron. The reduction in the power requirement comes from the high absorption cross sections of the ground state atoms and the preservation of the excitation within the interaction volume by resonance trapping.

The program at Los Alamos is directed at answering the most critical issues as early as possible as listed in Fig. 25. These include the geometric design of the neutralization chamber so the physical constraints can be understood and evaluated. Also high reflectivity mirrors must be developed and the means for evaluating them established. The thresholds for optical and particle

damage must be measured to ensure the compatibility of the mirrors in the system environment. Finally, the design and availability of high-powered lasers must be established.

In summary, laser-based neutralization of the ion beams offers many distinct advantages over other competing technologies. Among these, as listed in Fig. 26, are the high neutralization efficiency available with this process and the compact beam profile which is generated which produces very high intensities or current densities in the far field. Since the beam powers will be very large in the proposed applications, there will be a large region in the operational space where the beam can be increased more by increasing the power to the neutralizer lasers than the primary accelerator. The proof of principle of the process can be demonstrated, at low pulse repetition rate, with presently available high-energy lasers. High average power lasers for the eventual process application will require significant development. The efficiency and versatility of the laser process makes it the most promising technology for application to the final deployed neutral beam generator.

LASER NEUTRALIZER

OTIS G. PETERSON

FIG. 1

LASER NEUTRALIZER

CONTRIBUTORS

CLAUDE R. PHIPPS MICHAEL S. SOUKUP
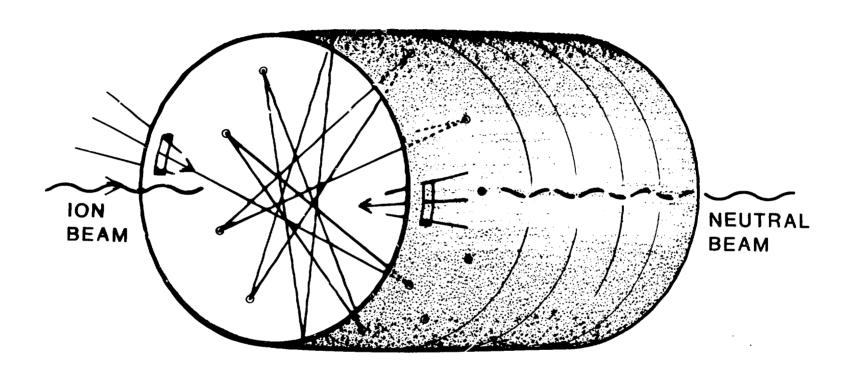
STEVEN R. FOLTYN NORMAN P. BARNES

HERBERT FLICKER ROY A. MICHELOTTI

MARK E. JOHNSON GLENN T. LINDHOLM

ROBERT SZE MIRIAM PACK

THOMAS SHAY WARREN HIGGINS, US ARMY

OTIS G. PETERSON

FIG. 2

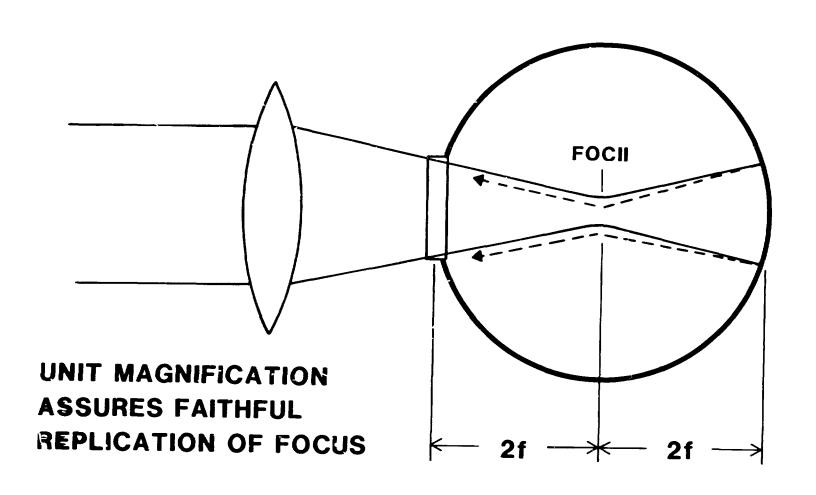# LASER NEUTRALIZER HAS
MANY ADVANTAGES

- LOW BEAM DIVERGENCE

- HIGH NEUTRALIZATION EFFICIENCY

- FOCUSABLE NEUTRALIZATION MEDIUM

- NO EFFLUENT NEAR BEAM PATH

- HIGH LEVERAGE

- NO FLUORESCENCE TO INTERFERE WITH
  BEAM SENSING

FIG. 3

CHM-VG-7984 A

NEUTRALIZATION CHAMBER
IS AN OPTICAL RELAY SYSTEM
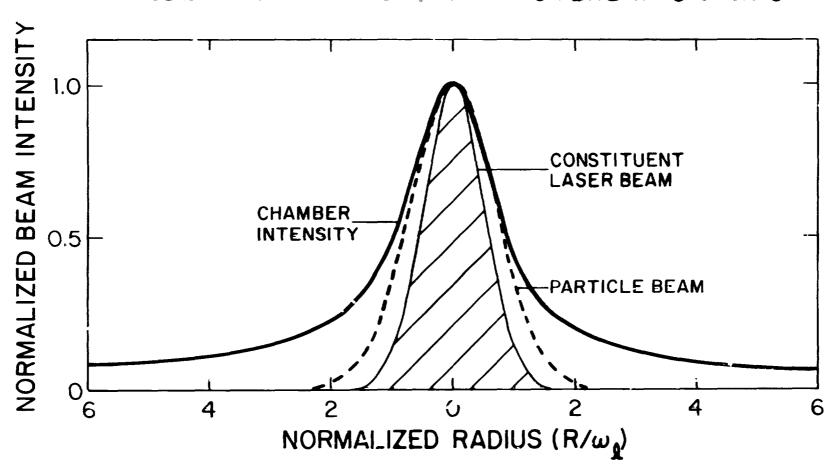
CYLINDRICAL GEOMETRY
PERMITS MULTIPLE INPUTS

FIG. 4

MC-8027
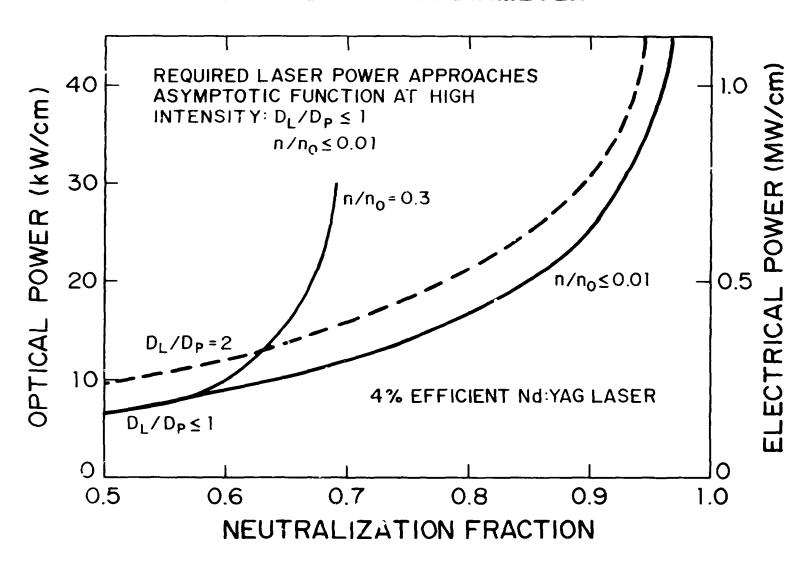
APLANATIC OPTICAL CHAMBER
ACCURATELY RELAYS BEAM FOCUS

FOCII

UNIT MAGNIFICATION
ASSURES FAITHFUL
REPLICATION OF FOCUS

2f   2f

FIG. 5

CHM-VG-8001
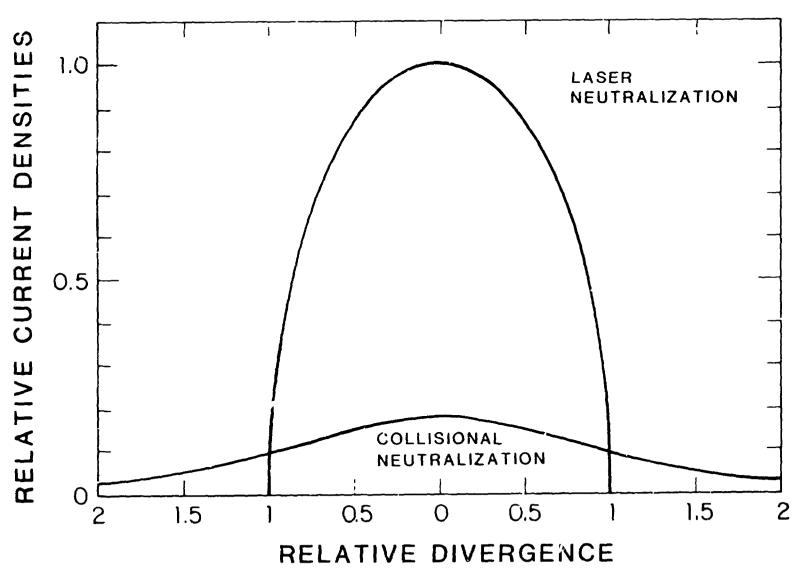
MULTiPASS NEUTRALIZER MAXIMIZES
LASER AND PARTICLE BEAM OVERLAP ON AXIS

NORMALIZED BEAM INTENSITY

1.0

0.5

0

CONSTITUENT
LASER BEAM

CHAMBER
INTENSITY

PARTICLE BEAM

6   4   2   0   2   4   6

NORMALIZED RADIUS (R/ω_ℓ)

FIG. 6

NEUTRALIZER LASER POWER NORMALIZED TO PARTICLE BEAM DIAMETER

REQUIRED LASER POWER APPROACHES ASYMPTOTIC FUNCTION AT HIGH INTENSITY: $D_L/D_P \leq 1$

$n/n_0 \leq 0.01$

$n/n_0 = 0.3$

$n/n_0 \leq 0.01$

$D_L/D_P = 2$

$D_L/D_P \leq 1$

4% EFFICIENT Nd:YAG LASER

OPTICAL POWER (kW/cm)

ELECTRICAL POWER (MW/cm)

NEUTRALIZATION FRACTION

FIG. 7

LASER NEUTRALIZATION DELIVERS
HIGHER INTENSITIES ON TARGET
THAN COLLISIONAL NEUTRALIZATION

FIG. 8

LASER NEUTRALIZATION MINIMIZES BEAM DIVERGENCE AND INCREASES CURRENT DENSITY ON TARGET

- PEAK CURRENT DENSITY INCREASED BY FACTOR OF FIVE (5)

  - INCREASED NEUTRALIZATION YIELDS FACTOR OF 1.6

  - REDUCED DIVERGENCE YIELDS FACTOR OF 3.3

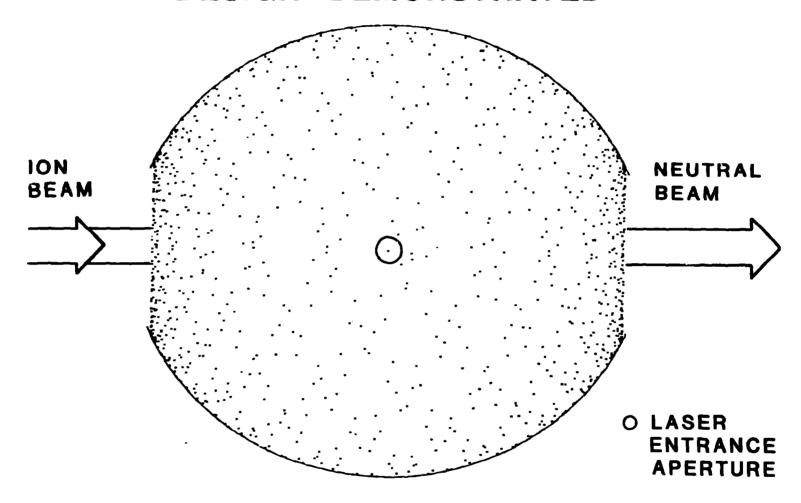- POLARIZED ILLUMINATION REDUCES DIVERGENCE 30% FROM UNPOLARIZED

CHM-VG-11,053

FIG. 9

LASER NEUTRALIZATION MINIMIZES BEAM DIVERGENCE

EXCITATION WAVELENGTH (μm)	ABSORPTION CROSS SECTION (10^{-16}cm^2)	DIVERGENCE (μrad)
1.06	0.4	1.07
1.6	0.2	0.56
1.75	0.1	0.42

CHM-VG-9918A

FIG. 17

THREE DIMENSIONAL OPTICAL DESIGN
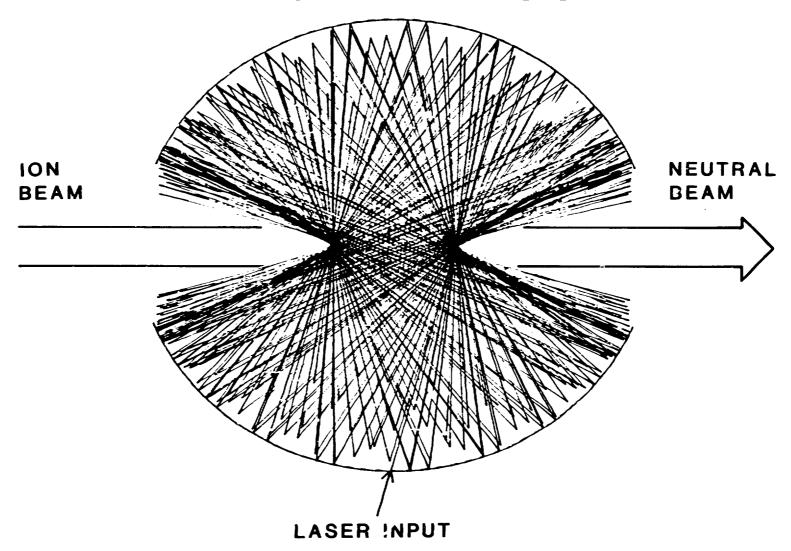# CODE IS OPERATIONAL

- **BEAM CONTAINMENT FOR 1,023 PASSES DEMONSTRATED**
  - CENTRAL RAY CALCULATIONS
  - 5% ECCENTRICITY ELLIPSE

- **CHAMBER DIMENSIONS 15x PARTICLE BEAM DIAMETER**
  - LASER BEAM DIAMETER 3/4 OF PARTICLE BEAM

- **CODE VALIDITY VERIFIED BY CALCULATIONS ON SPHERICAL GEOMETRIES**

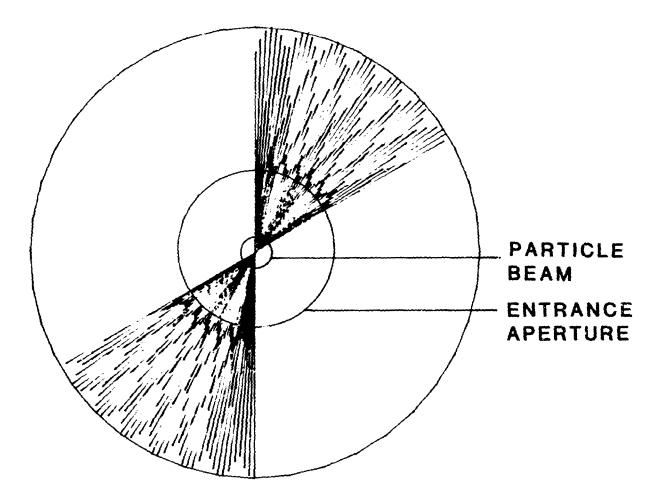FIG. 11   CHM — VG — 11,042

1023 PASS CONFINEMENT CAVITY
DESIGN DEMONSTRATED

ION
BEAM

NEUTRAL
BEAM

O LASER
ENTRANCE
APERTURE

● LASER BEAM (CENTRAL RAY) REFLECTIONS AT
NEUTRALIZER SURFACE : SHOWN AS DOTS

● ELLIPTICAL CROSS SECTION : 5% ECCENTRICITY

FIG. 12

CHM-VG-11,055

ELLIPTICAL GEOMETRY FOCUSES LIGHT INTO CENTRAL REGION

ION BEAM

NEUTRAL BEAM

LASER INPUT

● FIRST 250 PASSES OF CENTRAL RAYS

FIG. 13

CYLINDRICAL CHAMBER SENDS ALL
LASER BEAMS THROUGH CHAMBER AXIS

PARTICLE
BEAM

ENTRANCE
APERTURE

● FIRST 300 PASSES OF CENTRAL RAYS

FIG. 14

CHM-VG-11,058
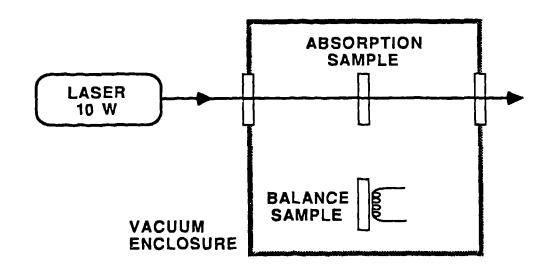
OPERATING OPTICAL TRANSPORT CODE ADVANCES DESIGN AND OPTIMIZATION PROGRAMS

- **PERMITS DESIGN OF LARGE "PASS-NUMBER" DEVICES**
  - RICH GEOMETRICAL PARAMETER SPACE TO BE EXPLORED
  - RAY PACKING DENSITY INCREASES POSSIBLE

- **EVALUATION OF BEAM FOCUSING**
  - CODE OPTION TRACES AUXILIARY RAYS
  - MULTIPLE FOCUSING AND ABERATIONS CAN BE EVALUATED

- **OPTICAL FIGURE REQUIREMENTS CAN BE EVALUATED**
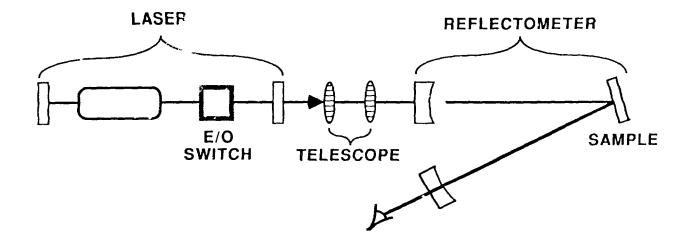 - FABRICATION TOLERANCES CAN BE DETERMINED

FIG. 15   CHM – VG – II,041

LASER CALORIMETER MEASURES PPM ABSORPTION

- **TEMPERATURE BALANCE GIVES ABSORBED POWER**
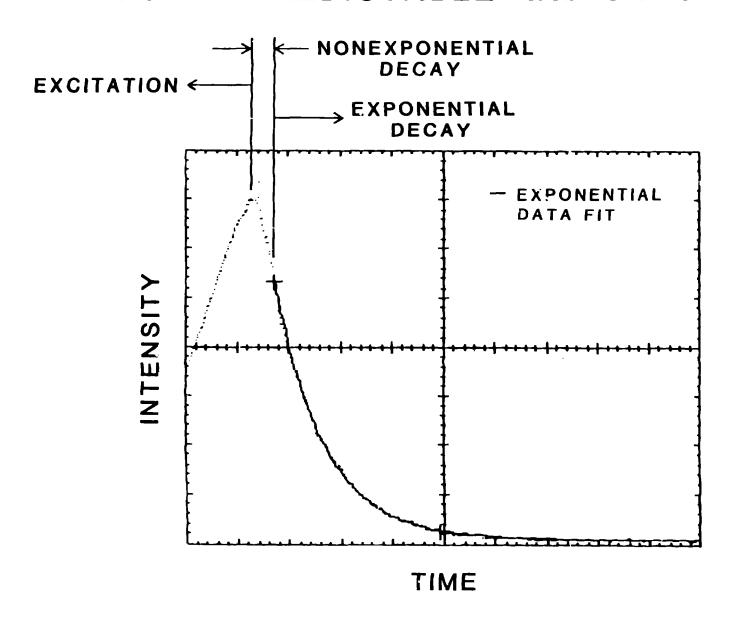   - ELECTRICAL POWER TO BALANCE SAMPLE EQUALS ABSORBED POWER
    - LOW MASS SUBSTRATES
    - MATCHED GEOMETRIES
    - LOW VACUUM / HIGH THERMAL ISOLATION

- **PPM ACCURACY FROM $10\mu W$ SENSITIVITY**

- **MEASURED 80 - 120 PPM ABSORPTION**
    - 99% REFLECTOR : 29 LAYER ZrO_2/SiO_2 ON FUSED SILICA
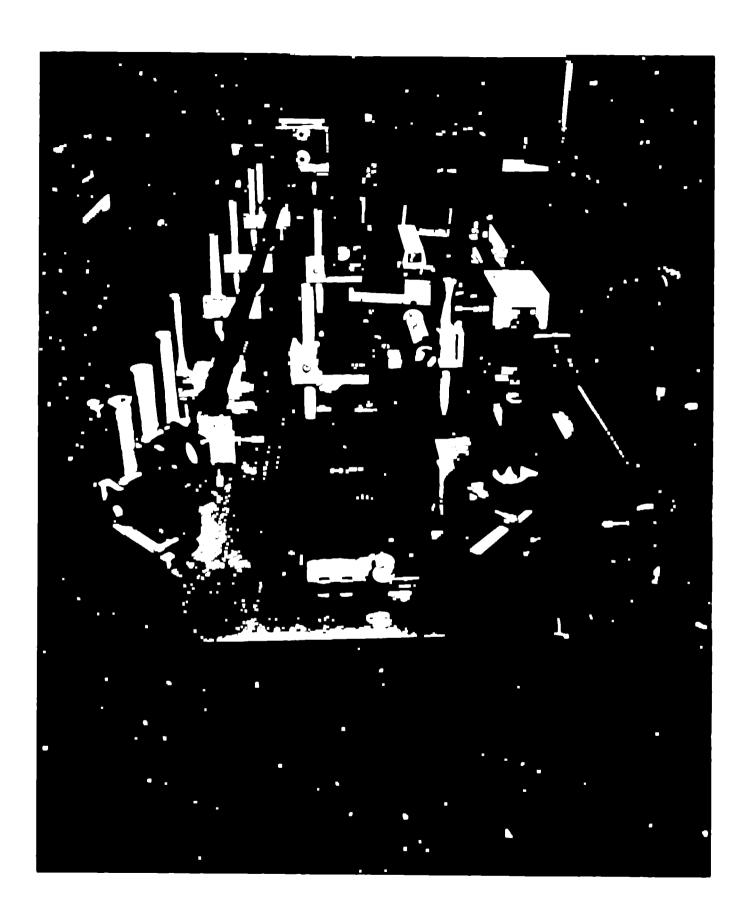
FIG. 16

CAVITY RING DOWN MEASURES
HIGH REFLECTIVITIES

- **REFLECTIVITY AND TOTAL LOSS MEASURED BY TEMPORAL DECAY OF TRAPPED LIGHT**
  - EXPONENTIAL DECAY = LENGTH / c / LOSS
  - LOSS OF 10^{-3}/ m GIVES $3 \mu s$ DECAY

- **SENSITIVITY LIMITED BY REFLECTOMETER MIRRORS AND LIGHT SWITCHING**
  - SAMPLE LOSS MEASUREMENT LIMITED TO 10% OF REFLECTOMETER MIRROR LOSSES
  - LIGHT SWITCH PLACED INTRARESONATOR TO KILL LASING AND ISOLATE FLUORESCENCE FROM REFLECTOMETER

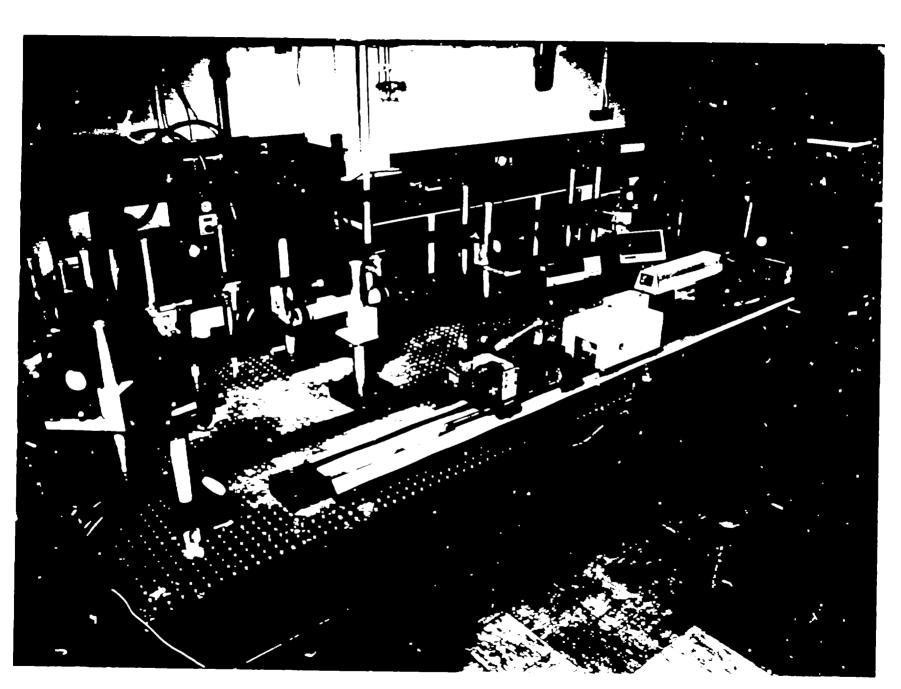# REFLECTOMETER PERFORMANCE
HIGHLY PREDICTABLE AND SENSITIVE

NONEXPONENTIAL
DECAY

EXCITATION

EXPONENTIAL
DECAY

— EXPONENTIAL
DATA FIT

INTENSITY

TIME

FIG. 18

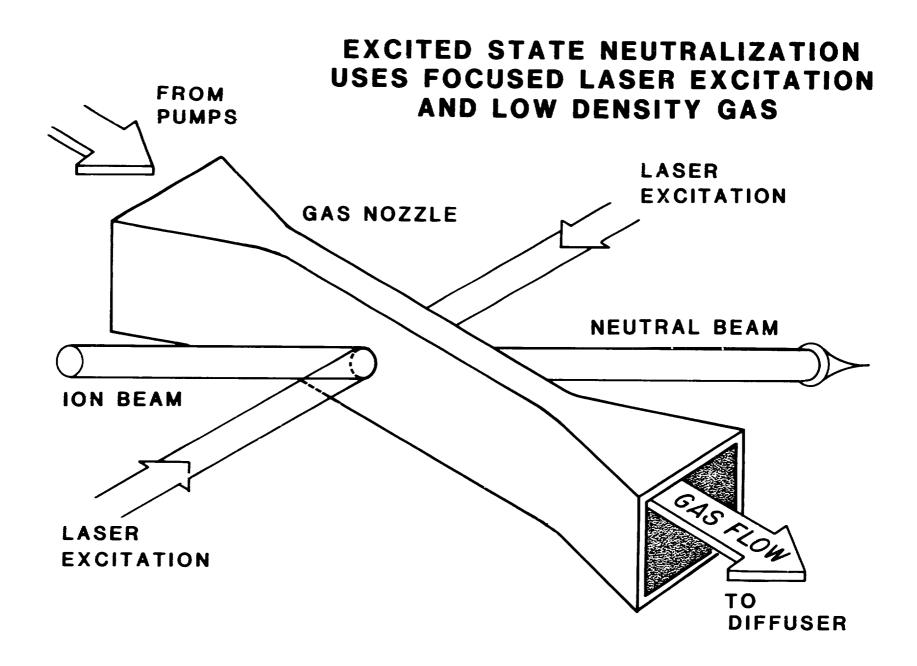FIG. 20

HIGH REFLECTIVITY MIRROR CHARACTERIZATION REQUIRE STATE-OF-THE-ART TECHNOLOGY

- **LASER CALORIMETER MEASURE ppm ABSORPTIONS**
  - NOW OPERATIONAL
  - TEST SAMPLES BEING EVALUATED

- **RING DOWN RESONATOR MEASURES TOTAL LOSS IN THE 10^{-3} OR LESS (0.999 or greater reflectivity) RANGE**
  - INSTRUMENT COMPONENTS OBTAINED
  - ASSEMBLY AND TEST IN PROGRESS

FIG. 21

CHM – VG – II,037

ADVANCED CONCEPT NEUTRALIZER COMBINES ADVANTAGES OF LASER AND COLLISION NEUTRALIZATION

LASER GENERATED EXCITED-STATE ATOMS ARE 10x BETTER THAN GROUND STATE ATOMS FOR NEUTRALIZATION AND USE 10x LESS LASER POWER THAN CONVENTIONAL LASER NEUTRALIZERS.

FIG. 22

EXCITED STATE NEUTRALIZATION USES FOCUSED LASER EXCITATION AND LOW DENSITY GAS

FROM PUMPS

GAS NOZZLE

LASER EXCITATION

NEUTRAL BEAM

ION BEAM

LASER EXCITATION

GAS FLOW

TO DIFFUSER

FIG. 23

CHM-VG-11,061

EXCITED-STATE NEUTRALIZERS HAVE LARGE POTENTIAL ADVANTAGES

- **ELECTRON DETACHMENT CROSS SECTIONS ARE PROBABLY 10x LARGER THAN GROUND STATE**

  - ORDER OF MAGNITUDE COLLISIONAL ENHANCEMENTS HAVE BEEN MEASURED AT LOW ENERGIES

  - HIGH ENERGY ENHANCEMENTS MUST BE VERIFIED

  - GAS FLOW REDUCE BY FACTOR OF 10

- **LASER ILLUMINATION IS EFFICIENTLY USED**

  - GROUND STATE ATOMS (Li, Na, etc.) HAVE HIGH ABSORPTION CROSS SECTIONS

  - EXCITATION PRESERVED BY RESONANCE TRAPPING

  - LASER POWER REQUIRED IS 2 kW/cm OF BEAM vs 10 - 20 kW/cm FOR CONVENTIONAL LASER NEUTRALIZER

- **PARTICLE BEAM DIVERGENCE IS REDUCED**

  - GAS DENSITY PER cm^2 REDUCED BY FACTOR OF 10

FIG. 24

LOS ALAMOS PROGRAM ADDRESSES
CRITICAL ISSUES

- **BEAM CONTAINMENT CHAMBER**

    - **TRANSPORT CODE FOR HIGH F-NUMBER, MULTIPASS OPTICAL SYSTEMS**

- **HIGH REFLECTIVITY MIRRORS**

    - **COATING DEVELOPMENT**

    - **RADIATION AND OPTICAL DAMAGE TESTING**

- **HIGH-POWER LASER DEVELOPMENT**

FIG. 25   CHM – VG – 9869

LASER NEUTRALIZER COMPLETES
OPTIMAL BEAM SYSTEM

- **MORE NEUTRAL BEAM CAN BE GENERATED BY ADDING POWER TO THE LASER THAN TO THE ACCELERATOR**

- **REDUCES DIVERGENCE**

  - ENHANCE RANGE

  - REDUCE POWER

  - REDUCE OUTPUT APERTURE

- **PROOF OF PRINCIPLE CAN BE DONE WITH PRESENT DAY TECHNOLOGY**

- **GREAT POTENTIAL FOR IMPROVEMENT WITH DEVELOPMENT**

FIG. 26

CHM – VG – 7993 A